Evaluation of Failure of Embankment Slope Constructed with Expansive Soils

Kuo Chieh Chao[1], Jong Beom Kang[2] and John D. Nelson[3]
[1]*Department of Civil and Infrastructure Engineering, Asian Institute of Technology, Bangkok, Thailand*
[2]*U.S. Bureau of Reclamation, Technical Service Center, Denver, Colorado, USA*
[3]*Engineering Analytics, Inc., and Colorado State University, Fort Collins, Colorado, USA*
E-mail: geoffchao@ait.asia

ABSTRACT: Slope failures in embankments constructed in expansive soils are often induced by rainfall infiltration during wet seasons or after a heavy rainfall event. Field investigations regarding the effect of rainfall infiltration on slope instability for expansive soil embankments indicate that shrinkage cracks developed during the drying and wetting cycles play an important role in slope instability. The excessive amount of infiltration through the shrinkage cracks decreases the matric suction of the expansive soil, and hence, results in a reduction of the shear strength of the soil accompanied with soil expansion, or heave. Furthermore, the modulus of elasticity of the soil decreases as water content increases and the soil heaves. The influence of these factors on the slope stability of expansive soil embankments is reviewed and discussed in the paper. Numerical modeling using the finite element computer programs SEEP/W and SIGMA/W was conducted to evaluate the volume change of an expansive soil embankment slope due to changes in suction arising from infiltration. Long-term stability of the expansive soil embankment slope was conducted using the computer program SLOPE/W. The expansive soil slope was also analyzed with a proposed remediation scheme to evaluate the effect of the remediation on long-term stability. The results of the numerical modeling for the slope with remediation were compared to those obtained for the slope without remediation. Furthermore, heaving of the expansive soil is accompanied by a reduction in the shear strength of the soil. Therefore, analysis of heave using the oedometer method was discussed in the paper. The results of the heave prediction using the oedometer method were compared to those obtained from the numerical modeling method. Reasons for the differences in amounts of predicted heave using both methods are discussed in the paper.

KEYWORDS: Expansive soil embankment slope, Heave prediction, Numerical modeling, Modulus of elasticity, Shear strength

1. INTRODUCTION

Embankments constructed with expansive soils often experience surficial slope failure induced by rainfall infiltration during wet seasons or after a heavy rainfall event. Field studies regarding the effect of rainfall infiltration on slope instability for expansive soil embankments have been conducted by several researchers (Ng et al., 2003; Wu and Huang. 2006; Zhan et al., 2007; Zheng et al., 2009). Most of these field studies concluded that surficial shrinkage cracks that were developed during the drying and wetting process play an important role in slope instability. The shrinkage cracks increase the amount of infiltration, and hence, increase the depth of wetting, resulting in a reduction of matric suction of the expansive soil. The reduction of matric suction decreases the shear strength of the soil. Besides the matric suction factor, heaving of the expansive soil due to hydration of adsorbed cations on the clay particles is accompanied with a reduction of the shear strength of the soil. In addition, the modulus of elasticity of the soil decreases as the water content increases and the soil heaves. The reduction in elastic modulus also increases the deformation of the soil. The discussion of these factors is presented in the paper.

Evaluation of the volume change of an expansive soil embankment slope due to changes in suction arising from infiltration was conducted using the finite element computer program SIGMA/W coupled with the SEEP/W computer program (GEO-SLOPE, 2007). Stability of the expansive soil embankment slope was also evaluated using the computer program SLOPE/W (GEO-SLOPE, 2007). The results of these analyses were presented to provide supported technical reasons for instability of the expansive soil slope during wet seasons or after a heavy rainfall event.

Soil stabilization measures are often utilized to enhance the stability of the embankment slopes constructed with expansive soils (McCleskey, 2005). A remediation approach proposed by Zheng et al. (2009) was analyzed to mitigate failures on expansive soil embankment slopes. Numerical modeling was conducted on the expansive soil slope with the proposed remediation approach. The results of the modeling conducted for the slope with remediation were compared to those obtained for the slope without remediation.

Heaving of the expansive soil and the resulting increase in void ratio plays an important role in the reduction of the shear strength of the soil. A commonly used heave prediction method, the oedometer method, is discussed in the paper. Heave prediction for the expansive soil embankment slope was conducted using the migration of the wetting front data obtained from the numerical modeling. The results of the heave prediction using the oedometer method were compared to those obtained from the numerical modeling method. Reasons for the differences in the amounts of predicted heave using the both methods are discussed in the paper.

2. LITERATURE REVIEW

2.1 Heave Prediction Methods

Heave prediction is generally accomplished by using one of two methods: (1) the soil suction method and (2) the oedometer method. Both methods take into account changes in soil suction and net normal stress but in different ways. In the soil suction method the suction is correlated through the soil-water characteristic curve (SWCC) with water content by an empirical equation and the stress is considered as a percentage of the swelling pressure. In the oedometer method, the stress is taken into account through the heave index, C_H, which is measured in the oedometer test and the suction is controlled by means of sample inundation in the oedometer test.

Methods of predicting heave using the soil suction method have been described by Miller et al. (1995) and McKeen (1992). Although the testing methods required for this method are not complex, nor difficult to perform, they are not normally conducted in ordinary geotechnical engineering laboratories. On the other hand, most geotechnical engineering laboratories routinely conduct oedometer tests or some variation of that test. Therefore, only the oedometer method will be discussed below.

2.1.1 Oedometer Tests

Various heave prediction methods based on results of one-dimensional oedometer tests have been developed (Fredlund et al., 1980; Department of the Army, 1983; Nelson and Miller, 1992;

Fredlund and Rahardjo, 1993; Fredlund et al., 2012). These methods utilize the net normal stress, $\sigma'' = (\sigma - u_a)$, and the matric suction; $\psi_m = (u_a - u_w)$ as the stress state variables. In these variables, σ is the total stress and u_a and u_w are the pore air and pore water pressures.

Two basic types of tests including the consolidation-swell (CS) test and the constant volume (CV) test are commonly performed for expansive soils. For the CS test, the sample is initially subjected to a prescribed vertical stress in the oedometer, and inundated under that constant vertical stress, σ''_i. The vertical strain that occurs due to wetting, termed the percent swell, $\varepsilon_{s\%}$, is measured, and the sample is usually subjected to an additional vertical load. The stress that would be required to restore the sample to its original height is termed the CS swelling pressure, σ''_{cs}. For the CV test, the sample is initially subjected to a prescribed vertical stress, but during inundation the sample is confined from swelling and the stress that is required to prevent swell is measured. This is termed the CV swelling pressure, σ''_{cv}. The results of the CS and CV tests are normally plotted in the form of vertical strain as a function of the applied stress. The typical two-dimensional forms of each test are shown in Figure 1.

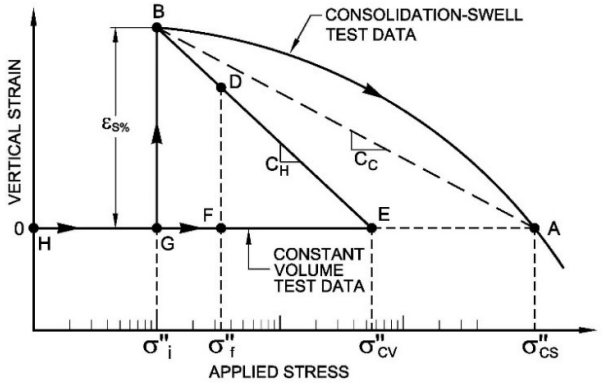

Figure 1 Oedometer test results and determination of heave index, C_H (Nelson et al., 2015)

In consideration of the fact that the constitutive relationship is three-dimensional in nature as shown in Figure 2, the actual stress paths are three-dimensional in nature as well. The stress paths for the CS and CV tests are shown in Figure 2. For the CS test, the initial state of the soil in an oedometer test is represented by the point labeled K in Figure 2. At that point the soil suction is equal to a value designated as ψ_{m1}. The net normal stress is that at which the sample will be inundated, i.e., the inundation stress, σ''_i. When the sample is inundated, the suction is reduced to ψ_{mo} and the soil swells along the path KB. The projection of that stress path on the plane defined by the axes for $\varepsilon_{s\%}$ and log σ'' is the line GB. The sample is then loaded back to its original height along the path BA. The value of stress corresponding to point A is the CS swelling pressure, σ''_{cs}.

In the CV test, the initial state of stress is also at point K, but because it is constrained from swelling it develops a confining stress as the suction decreases to ψ_{mo} and the stress path would be along a line such as KE. The value of stress corresponding to point E is the CV swelling pressure, σ''_{cv}. Due to hysteretic effects, the value of σ''_{cv} is generally less than that of σ''_{cs}. The reason for this is somewhat intuitive in that it should be easier to prevent water molecules from entering into the soil lattice than to force the water out once it has entered into the soil. Factors contributing to hysteresis were discussed in Nelson et al. (2015).

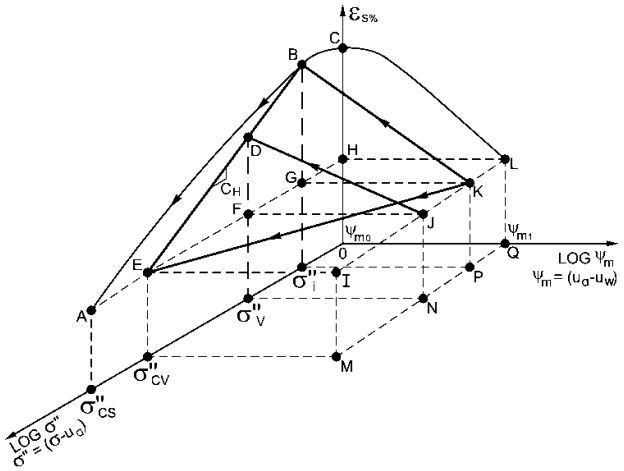

Figure 2 Stress path for soil expansion (Nelson et al., 2015)

2.1.2 Heave Prediction Equations

The equation for predicting heave using the oedometer method is based on the fundamental definition of strain as seen in Equation (1).

$$\varepsilon_s = \frac{\varepsilon_{s\%}}{100} = \frac{\Delta H}{H} \tag{1}$$

where: ε_s = strain in the layer that is heaving,
$\varepsilon_{s\%}$ = percent swell that will occur when that stratum becomes wetted (strain in percent),
H = thickness of a layer of soil, and
ΔH = change in thickness of that layer due to heave.

To obtain the basic equation for heave of a soil layer, Equation (1) must be solved for ΔH, as seen in Equation (2).

$$\Delta H = \varepsilon_s H = \frac{\varepsilon_{s\%} H}{100} \tag{2}$$

The strain, ε_s or $\varepsilon_{s\%}$, in Equation (2) is the strain that will result in the soil due to an increase in water content. It is also a function of the vertical stress that exists in the stratum at the time it becomes wetted. Therefore, it is necessary to develop a relationship between the amount of swell that a soil will experience when wetted, and the stress that is applied at the time of wetting. It has been shown that the relationship between the percent swell and the applied stress can be represented by a linear relationship as defined by the line BDE shown in Figure 1 (Nelson et al., 2006 and 2012). The heave index, C_H, is the slope of that line and is given by Equation (3). It is shown in Equation (3) that the value of C_H can be determined from the results of a consolidation-swell test (i.e. $\varepsilon_{s\%}$ and σ''_i) and a constant volume test (i.e. σ''_{cv}) using identical samples of the same soil. In practice, it is virtually impossible to obtain two identical samples from the field. Consequently, it is convenient to develop a relationship between the CS swelling pressure, σ''_{cs}, and the CV swelling pressure, σ''_{cv}. The relationship between σ''_{cs} and σ''_{cv} will be discussed later in this section.

$$C_H = \frac{\varepsilon_{s\%}}{100 \times \log\left[\frac{\sigma''_{cv}}{\sigma''_i}\right]} \tag{3}$$

where: $\varepsilon_{s\%}$ = percent swell corresponding to the particular value of σ''_i expressed as a percent, and
σ''_i = vertical stress at which the sample is inundated.

Equation (4) can be obtained from Equation (3).

$$\varepsilon_s = \frac{\varepsilon_{s\%}}{100} = C_H \log\left[\frac{\sigma''_{cv}}{\sigma''_f}\right] \tag{4}$$

Equation (4) can be substituted into Equation (2) to give,

$$\Delta H = C_H H \log\left[\frac{\sigma''_{cv}}{\sigma''_f}\right] \tag{5}$$

For practical applications, a soil profile divided into layers of thickness H must be considered, and the value of heave for each layer computed. Adding the incremental values gives the total free-field heave, ρ. The general equation for predicting free-field heave is shown in Equation (6).

$$\rho = \sum_{i=1}^{n} \Delta H_i = \sum_{i=1}^{n} \left\{ C_H H \log\left[\frac{\sigma''_{cv}}{\sigma''_f}\right] \right\}_i \tag{6}$$

where: ρ = total free-field heave,
ΔH_i = heave of layer i,
C_H = heave index of layer i,
H_i = initial thickness of layer i ,
σ''_{cv} = constant volume swelling pressure of layer i, and
σ''_f = final vertical net normal stress at the midpoint of layer i.

2.1.2.1 Relationships Between σ''_{cv} and σ''_{cs}

A number of investigators have proposed relationships between σ''_{cv} and σ''_{cs} (Edil and Alanazy, 1992; Reichler, 1997; Bonner, 1998; Thompson et al., 2006; Nelson et al., 2006; and Nelson et al., 2012). Those investigators have generally proposed some form of equation that uses a simple ratio between σ''_{cv} and σ''_{cs}. Nelson and Chao (2014) proposed another approach derived by observations of oedometer test results from a series of tests performed on identical samples. A series of oedometer tests performed on the same soil at different σ''_i values show that the test results will have the form shown in Figure 3 (Gilchrist, 1963; Reichler, 1997). Figure 3 shows that as σ''_i increases, the swelling pressure obtained in the CS test decreases. If the soil does not swell when it is inundated, i.e., a CV oedometer test, the inundation stress would correspond to the swelling pressure. Therefore, if σ''_{cs} is plotted against σ''_i, the value of σ''_{cs} will converge to σ''_{cv} at the point where σ''_i is equal to σ''_{cv}, as shown in Figure 4. In that figure, the values of σ''_{cs1}, σ''_{cs2}, and σ''_{cs3} are plotted against the corresponding values of σ''_{i1}, σ''_{i2}, and σ''_{i3}. Point M in Figure 3 corresponds to point M in Figure 4 and represents the point where σ''_i equals σ''_{cv}. This point plots on a line with a slope of 1:1 in Figure 4. It represents the point where the soil was wetted at an inundation stress that is equal to the CV swelling pressure. Data for remolded soils taken from Gilchrist (1963) and Reichler (1997) confirm the idealized form shown in Figure 3.

The equation of the line in Figure 4 can be written as Equation (7).

$$\frac{\log\sigma''_{cs} - \log\sigma''_{cv}}{\log\sigma''_{cv} - \log\sigma''_i} = m \tag{7}$$

where: m = slope of the line.

Note that the value of "m" is the absolute value of the slope of the line in Figure 4, and thus, is positive. Equation (7) can be rewritten to obtain the relationship between σ''_{cs} and σ''_{cv} as:

$$\log\sigma''_{cv} = \frac{\log\sigma''_{cs} + m \times \log\sigma''_i}{1+m} \tag{8}$$

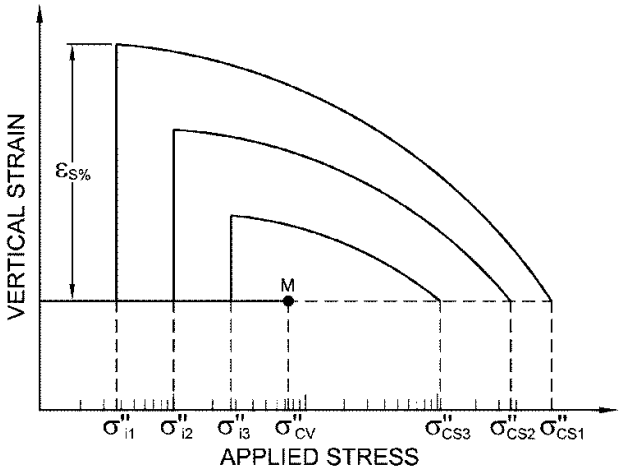

Figure 3 Idealized oedometer test results for different values of σ''_i (Nelson and Chao, 2014)

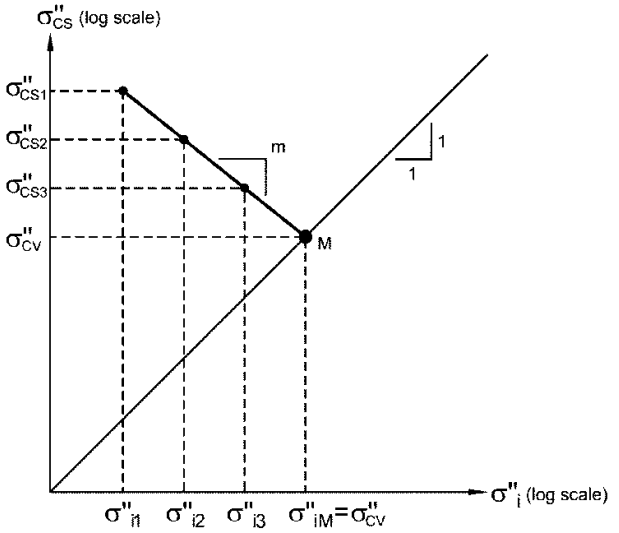

Figure 4 Convergence of σ''_{cs} and σ''_i to σ''_{cv} (Nelson and Chao, 2014)

The parameter m depends on the particular soil, its expansive nature, and other properties of the soil. Nelson and Chao (2014) compiled a database of corresponding values of σ''_{cs} and σ''_{cv} based on various sources including their own data, review of many soils reports, and values published in the literature (Gilchrist, 1963; Porter, 1977; Reichler, 1997; Feng et al., 1998; Bonner, 1998; Fredlund, 2004; Al-Mhaidib, 2006; Thompson et al., 2006). The types of the soils that were analyzed included claystone, weathered claystone, clay, clay fill, and sand-bentonite.

Figure 5 shows values of m for each sample sorted according to the value of m. The data indicate that all values of m fall below 2. In Figure 5, there appear to be two groups of data. The values for the clay tend to be grouped at lower values than those or the claystone

or shale. Nelson and Chao (2014) indicated that this is due to physicochemical differences and the existence of diagenetic bonds in the highly overconsolidated claystone and shale.

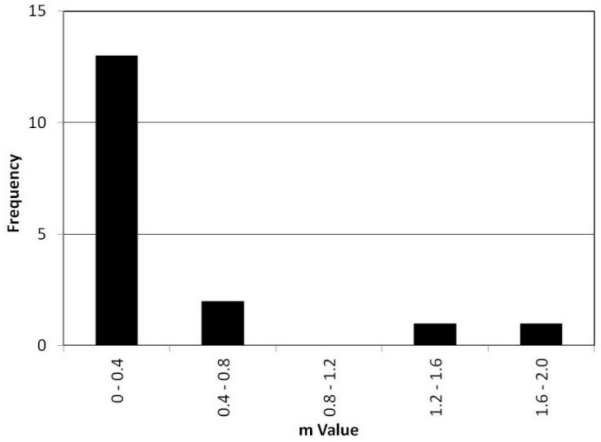

(a) Clay (Undisturbed), Fill, or Remolded

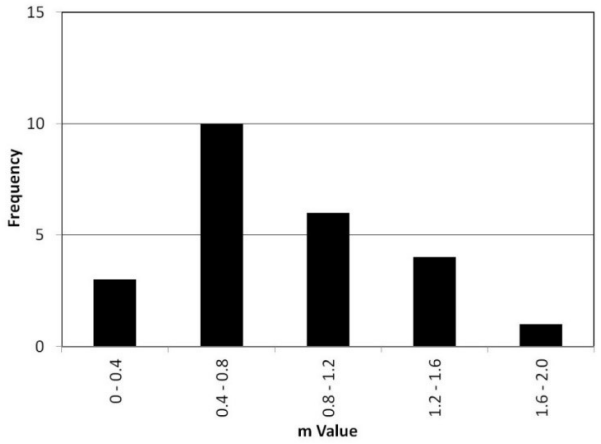

(b) Claystone or Shale (Undisturbed)

Figure 5 Histogram for values of m: (a) undisturbed clay, remolded clay or claystone; (b) undisturbed claystone or shale (Nelson and Chao, 2014)

Nelson and Chao (2014) performed a sensitivity test of the m value on the predicted free-field heave and concluded that the computed heave is not overly sensitive to the value of m. It was observed that if the value of m is varied outside of the appropriate range, the predicted heave will be more sensitive to the value of m. However, the ranges of values for particular soils are sufficiently broad. Values for a particular soil type or geological area can be determined by careful testing of a number of samples of the same soil.

2.1.2.2 Percent Swell and Swelling Pressure for Partially Wetted Soils

For partially wetted soils, it is necessary to modify the fully wetted oedometer data to determine the values of percent swell and swelling pressure to be used to predict heave. Figure 6 shows normalized percent swell plotted against degree of saturation for various values of the initial degree of saturation (Chao, 2007). The normalized percent swell was determined by dividing the values of percent swell that occurred at a particular degree of saturation by the maximum values of percent swell at full wetting in an oedometer test. These curves can be used to calculate the percent swell for a partially wetted soil using the results of a fully wetted soil in the consolidation-swell test.

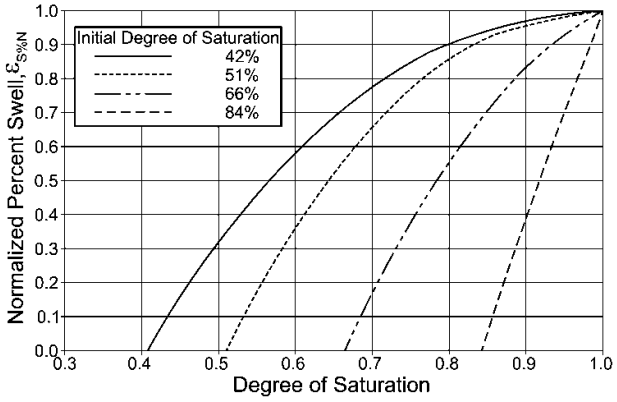

Figure 6 Normalized percent swell vs. degree of saturation (modified from Chao, 2007)

In addition to determining a value for the percent swell at partial wetting, the swelling pressure for a partially wetted soil must also be determined. Reichler (1997) indicated that an e-log p curve from a partially wetted CS test has the same shape as that from a fully wetted CS test. This suggests a procedure for determining a value of reduced swelling pressure, σ''_{cvN}, to be used for computing heave in a partially wetted soil, as shown in Figure 7. To determine the reduced swelling pressure a line is drawn parallel to the CH line and passing through the value of normalized percent swell, $\varepsilon_{s\%N}$, that was determined by Figure 6. Where that line intersects the axis for zero swell is the reduced swelling pressure, σ''_{cvN}.

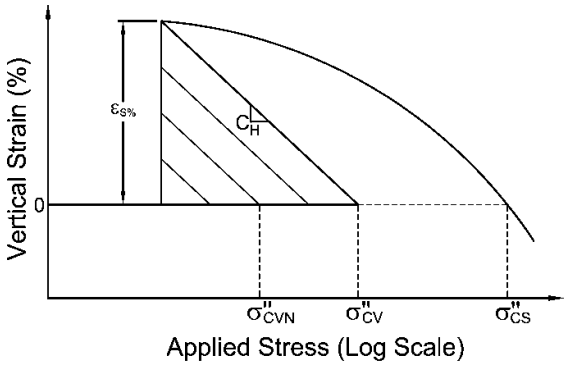

Figure 7 Procedure for determining swelling pressure for partially wetted soil (Nelson et al., 2015)

2.2 Modulus of Elasticity

Modulus of elasticity, E, of soils is an important parameter for evaluating elastic deformation of expansive soil embankments. Practicing engineers generally assume a constant value of E that has been determined from laboratory testing. However, the value of E varies in response to a change in matric suction and net normal stress. Therefore, E should be determined for the entire range of the constitutive surface that is expected to occur during the design life of the embankment. The value of E at the in situ condition prior to wetting can be calculated from unconfined compression (UC), triaxial, or oedometer tests performed at the in situ water content. The value of E at near saturated conditions can be determined using results of triaxial or oedometer tests.

Vu and Fredlund (2006) evaluated the modulus of elasticity property for Regina clay. Figure 8 illustrates the results of their evaluation and indicates that modulus of elasticity is a function of the net normal stress and matric suction. Vu and Fredlund (2006) noted that the modulus of elasticity is only a function of matric suction when the initial net normal stress is unchanged. During the heaving process of an expansive soil due to wetting, the increase in vertical stress due to the soil self-weight is insignificant. Therefore, when analyzing a slope in expansive soil, it is necessary to consider the change in the modulus of elasticity only as a function of matric suction.

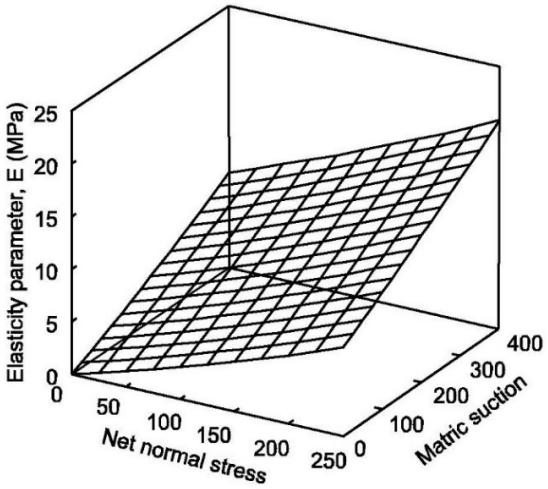

Figure 8 Elasticity parameter function for Regina clay (Vu and Fredlund, 2006)

The authors have also developed a method to determine the modulus of elasticity for a variety of soils using data obtained from CS tests. The CS testing procedure comprised two loading sequences. Initially the sample was loaded to the inundation stress under natural water content conditions. This portion of the curve was used to determine the constrained modulus, D, under relatively dry conditions. After the sample had been inundated and allowed to swell, it was loaded back to the point where the sample was the same height as it was when inundation was started. This portion of the curve was used to determine the values of D at various stress levels for almost saturated conditions. The relationship between E and D is presented in Lambe and Whitman (1969) as well as many other books on mechanics of materials.

Numerous tests were run to determine the elastic modulus of sandy clay, weathered claystone, claystone, and shale. These tests were run using both the UC and oedometer testing methods. The elastic modulus for each soil/rock type was plotted versus degree of saturation to determine if a relationship existed between elastic modulus and the degree of saturation. These plots are presented on Figures 9(a) through 9(d).

Figures 9(a) through 9(d) indicates that the values of E range from approximately 2 to 16 MPa for the soils tested using the oedometer test method. The computed E values based on the oedometer test results are consistent with those measured from the unconfined compression tests for samples at near-saturated conditions. The data shown in Figures 9(a) through 9(d) are compatible with the planar nature of the surface shown in Figure 8. The Young's modulus for partially saturated soil can be estimated based on interpolation between the value measured at saturation and that at the in situ water content.

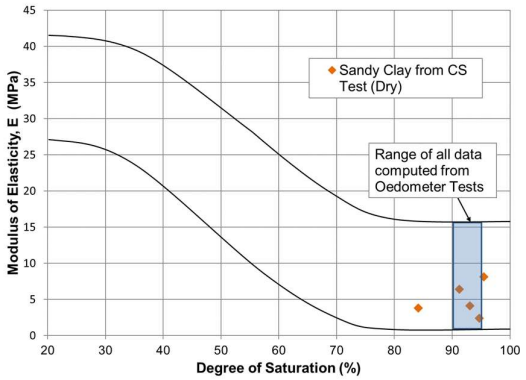

(a) Sandy Clay

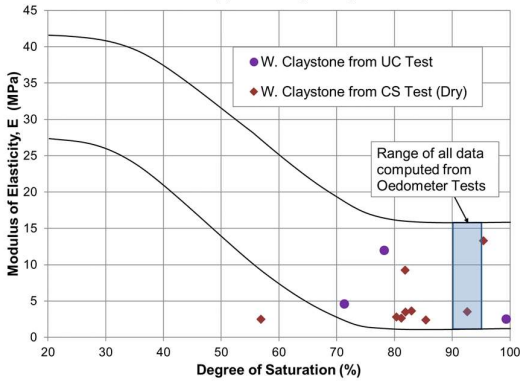

(b) Weathered Claystone

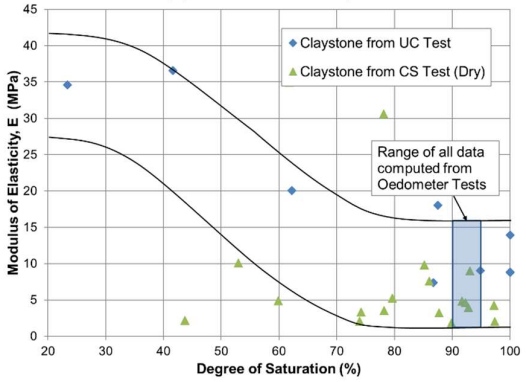

(c) Claystone

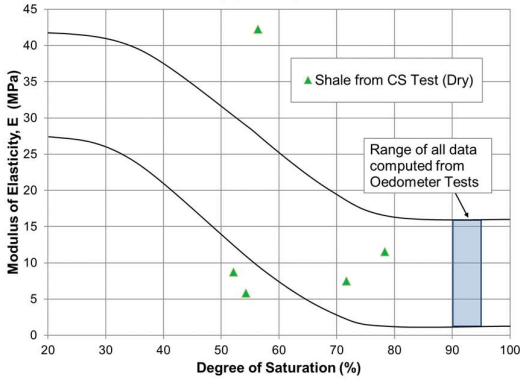

(d) Shale

Figure 9 Effect of degree of saturation on modulus of elasticity: (a) sandy clay; (b) weathered claystone; (c) claystone; and (d) shale

2.3 Shear Strength

The amount of research regarding the shear strength behavior of expansive soils is limited. In general, the research indicates that the shear strength of expansive soils reduces with an increase in moisture content (Sherif et al., 1984; Darrg, 1984; Katti et al., 2002; Miao et al., 2007; Al-Mhaidib and Al-Shamrani, 2006; Zhan and Ng, 2006; Elkady and Abbas, 2012). Darrg (1984) attributed the reduction in shear strength during swelling to a reduction in cohesion rather than a change in angle of internal friction. Katti et al. (2002) indicated that the shear strength for expansive soils may be linear or bilinear depending on the initial void ratio of the samples. Miao et al. (2007) evaluated the effect of initial degree of saturation on the shear strength of expansive soils and concluded that shear strength decreases with an increase in the initial degree of saturation. Al-Mhaidib and Al-Shamrani (2006) conducted triaxial tests on expansive shale samples in order to evaluate the change in the shear strength of the soil as related to the amount of swell. Figure 10 shows the results of their tests. This figure indicates that the shear strength of the soil can be related directly to the amount of swell, both of which are functions of the degree of wetting. The shear strength of the fully swelled samples was approximately 10% of the shear strength of the non-swelled samples.

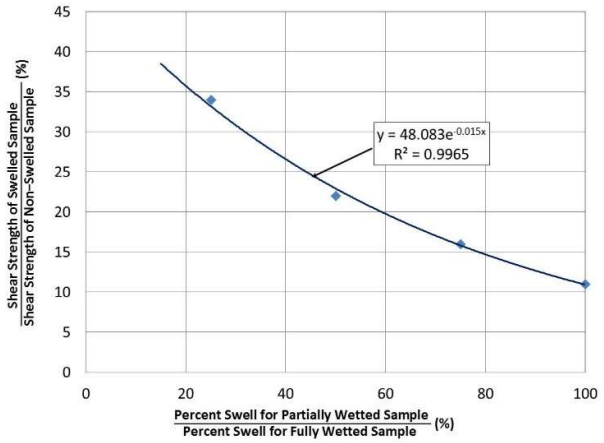

Figure 10 Effect of Swell on Shear Strength of Expansive Soils (modified from Al-Mhaidib and Al-Shamrani, 2006)

Expansive soils can be considered within the realm of unsaturated soils. Fredlund et al. (1978) provided the following linear form to express the shear strength of an unsaturated soil in terms of two independent stress state variables:

$$\tau_{ff} = c' + (\sigma_f - u_a)_f \tan\phi' + (u_a - u_w)_f \tan\phi^b \quad (9)$$

where: c' = effective cohesion,
$(\sigma_f - u_a)_f$ = net normal stress state on the failure plane at failure,
ϕ' = angle of internal friction,
$(u_a - u_w)_f$ = matric suction on the failure plane at the failure, and
ϕ^b = angle indicating the rate of increase in shear strength relative to the matric suction.

Zhan and Ng (2006) performed suction-controlled direct shear tests on expansive silty clay. Their experimental results show that the dilatancy of the expansive clay increases with an increase in the applied suction for the samples. Zhan and Ng (2006) concluded that matric suction contributes to the shear strength of the expansive soil via two different mechanisms: (1) the contribution of capillary force to interparticle normal stress and (2) the effect of suction on soil dilatancy. To account for the effect of suction on soil dilatancy, Zhan and Ng (2006) added the dilation angle, ϕ^d, into the shear strength equation proposed by Fredlund et al. (1978) as follows:

$$\tau_{ff} = c' + (\sigma_f - u_a)_f \tan(\phi' + \phi^d) + (u_a - u_w)_f \tan\phi^b \quad (10)$$

Zhan and Ng (2006) indicated that the value of ϕ^d is not only a function of soil state and soil structure, but also depends on the matric suction value.

3. NUMERICAL MODELING

3.1 General

Evaluation of the volume change of an expansive soil embankment slope due to changes in suction arising from infiltration was conducted using the finite element computer programs SEEP/W and SIGMA/W (GEO-SLOPE, 2007). Analyses considered an expansive embankment slope both without and with remediation. SEEP/W analyzes groundwater seepage and excess pore-water pressure dissipation problems within porous materials. SEEP/W can model both saturated and unsaturated flow. SIGMA/W is a finite element program that can be used to analyze stress and deformation analyses of earth structures. SIGMA/W can perform a simple linear elastic deformation analysis or a highly sophisticated, nonlinear elastic-plastic effective stress analysis. SIGMA/W is fully coupled with SEEP/W in this study. In the coupled approach, SEEP/W calculates transient pore-water pressure changes due to precipitation, while SIGMA/W calculates deformations resulting from the pore-water pressure changes.

Evaluation of the stability of the expansive soil slope was conducted using the computer program SLOPE/W (GEO-SLOPE, 2007). SLOPE/W was used to calculate the minimum factor of safety of the slope with time resulting from the increase in pore-water pressure, and the reduction of the shear strength of the soil due to wetting.

3.2 Cross Sections Analyzed

A hypothetical expansive soil embankment slope without remediation used in this study is shown in Figure 11. The embankment slope consists of highly plastic clay, and is 12 meters high with a 1.75H:1V slope. Various degrees of weathering of the clay materials with depth due to a drying and wetting process were considered when determining soil layers and the hydraulic conductivity (see Section 3.3). The embankment slope was divided into three layers, each of which has different material properties. The top two layers of the cross section are each 3 meters in height, and the lowest layer of the clay was assumed to extend to the bottom of the cross section.

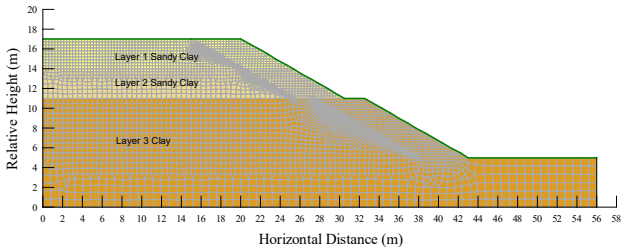

Figure 11 Hypothetical cross section without remediation

Expansive soil embankment slopes are known in China to have shallow slope failures during wet seasons or after a heavy rainfall event. A hypothetical expansive soil slope that was constructed with a stabilization approach of the nature proposed by Zheng et al. (2009) was analyzed in the paper. A flexible reinforced structure was proposed by Zheng et al. (2009) to stabilize and protect the cut

slopes in expansive soils. The flexible reinforced structure consists of moisture-conditioned and compacted on-site expansive fill with geogrid reinforcement. The geogrids are sandwiched between the layers of the compacted expansive fill materials. The flexible reinforced structure was assumed to be 5 meters in width. A drain system is constructed at the bottom of the flexible reinforced structure. Figure 12 shows the geometry of the cut slope with the flexible reinforced structure. Zheng et al. (2009) indicated that this approach can be constructed easily and is cost effective compared to other rigid reinforced structure approaches.

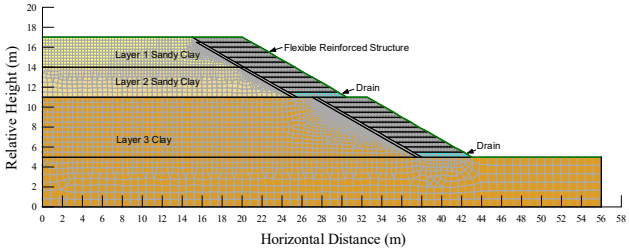

Figure 12 Hypothetical cross section with remediation

3.3 Material Properties and Boundary Conditions Used in the Analyses

Soil properties used in the analyses are listed in Table 1. In general, the soil properties were obtained from laboratory testing, literature, or our experience. The soil-water characteristic curves (SWCCs) for the materials used in the analyses were provided by Dr. Zhang of Changsha University of Science and Technology (CSUST), Changsha, Hunan, China and are shown in Figure 13. The values of the saturated hydraulic conductivity (K_{sat}) for the materials were also provided by CSUST. It should be noted that the K_{sat} value for the top and middle layer was assumed to be two and one order of magnitude higher, respectively, than that of the lowest layer in order to simulate the effect of surface shrinkage cracks. The hydraulic conductivity functions for the materials were determined from the SWCCs and the K_{sat} values of the materials using the Fredlund et al. (1994) equation.

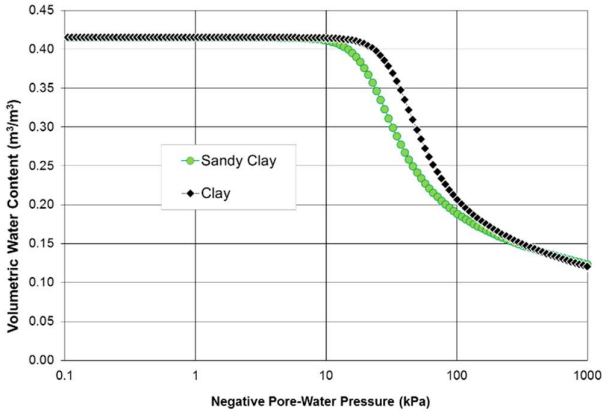

Figure 13 Soil water characteristic curves for the materials used in the analyses

The value of E at near saturation for the materials was estimated to be 1.5 MPa using the oedometer test approach presented above. The oedometer test data were provided by CSUST for the materials. The value of E for the initial water content conditions was estimated to be 2.5 MPa based on the relationship of E vs. degree of saturation shown in Figure 9(a).

Zhan et al. (2007) conducted an experiment to produce rainfall artificially using a sprinkler system designed for an expansive soil slope. The amount of infiltration that they determined for a simulation of low rainfall intensity was 3 mm/hour. Therefore, the infiltration was specified as a flux boundary equal to 3 mm/hour along the ground surface in this study. The groundwater table was assumed to be 17 meters below the top of the cross section. The initial suction of the soils above the groundwater table was specified to be 28 kPa based on the observed initial water content values shown in Table 1.

Table 1 Summary of soil properties of the materials used in the analyses

Soil Property	Layer 1 (Sandy Clay)	Layer 2 (Sandy Clay)	Layer 3 (Clay)
Initial Water Content (%)	23	23	23
Total Unit Weight (kN/m^3)	20	20	20
Sat. Hydraulic Conductivity (m/sec)	1×10^{-7}	1×10^{-8}	1×10^{-9}
Effective Cohesion (kPa)	7	7	23
Effective Angle of Internal Friction (degrees)	23	23	15
Angle of Internal Friction Due to Suction (degrees)	10	10	10
Poisson's Ratio	0.334	0.334	0.334

3.4 Results of Analyses

3.4.1 Performance of Slope Without Remediation

The analyses of SIGMA/W coupled with SEEP/W were conducted to observe the swelling clay behavior due to changes in matric suction as the transient wetting front advances into the ground. Figure 14 shows the migration of the wetting front for the embankment slope without remediation 4 years after the start of the infiltration. This figure shows that in a period of 3 years the wetting front migrates to a depth of about 11 meters below the top of the ground surface. The model was run to simulate a 10 year period. For the amount of the infiltration specified at the ground surface at the end of about 8 years, most of the cross section was saturated. Figure 15 presents the resulting deformed mesh that depicts heave at the end of 10 years due to the reduction of soil suction for the cut slope. The change of heave with time along the ground surface obtained from the coupled analyses is presented in Figure 16. Review of the results shown in Figure 16 suggests that most of the heave occurred in the first 8 years after wetting commenced. A maximum heave of about 114 mm and 75 mm took place at the top and middle of the cut slope, respectively.

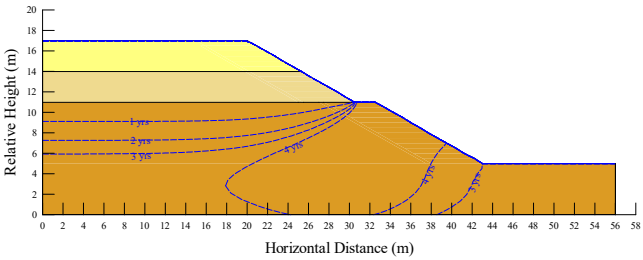

Figure 14 Wetting front migration for the embankment slope without remediation

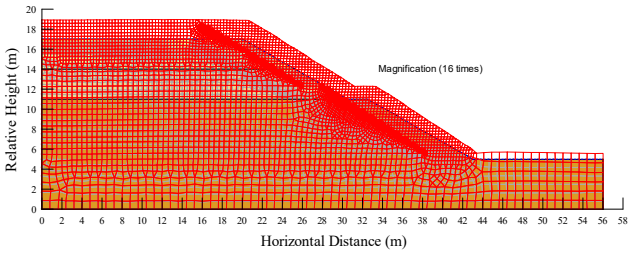

Figure 15 Deformed mesh due to changes in matric suction for the embankment slope without remediation

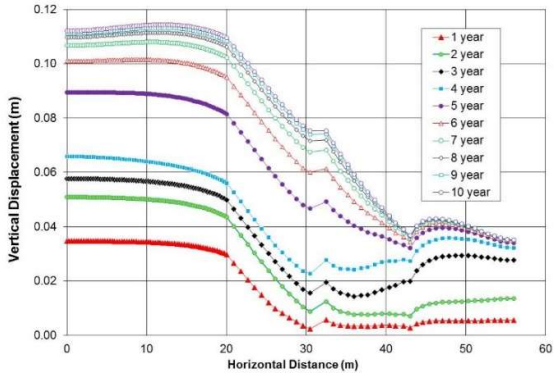

Figure 16 Change of heave with time along the ground surface for the embankment slope without remediation

The results of the SEEP/W and SIGMA/W analyses were input into SLOPE/W to evaluate the stability of the cut slope due to the migration of the wetting front. Figure 17 shows the minimum factor of safety with time for the cut slope without remediation after the introduction of the infiltration. Figure 17 suggests that the minimum factor of safety of the slope decreases to a value below 1.0 within approximately 40 days after the start of the infiltration. This is consistent with the observation of the slope failures made by Zheng et al. (2009). They indicated that slope failures usually occurred late in the rainy season or following a heavy rain. It is also seen from our SLOPE/W model that the slope failures took place in a shallow layer at a depth of approximately 3 meters from the top of the ground surface. This is also consistent with the depths of the slope failures that Zheng et al. (2009) observed.

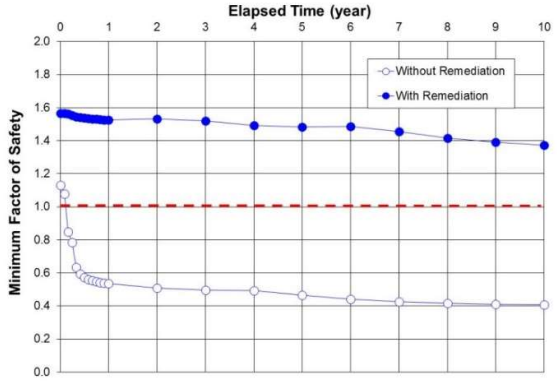

Figure 17 Minimum factor of safety with time for the embankment slope without and with remediation

3.4.2 Performance of Slope With Remediation

The coupled SIGMA/W and SEEP/W analyses were also conducted for the embankment slope constructed with the flexible reinforced structure remediation approach discussed above. The wetting front migration for the embankment slope with remediation 10 years after the start of the infiltration is presented in Figure 18. Figure 19 presents the resulting deformed mesh that depicts heave due to the reduction of the soil suction. Figure 20 shows the change of heave with time along the ground surface obtained from the coupled analyses. Comparison of the water migration results shown in Figures 14 and 18 shows that the pore water pressure was reduced significantly within the remediated slope area due to the installation of the drain system. The maximum heave within the remediated slope area that could occur is also reduced significantly resulting from the remediation of the cut slope, as shown by comparison of Figures 16 and 20.

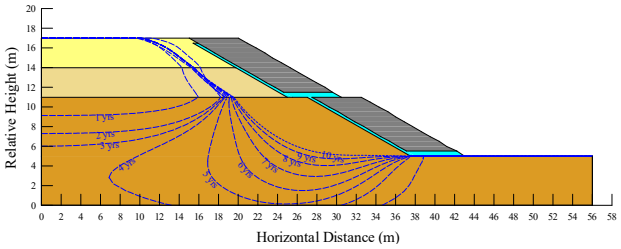

Figure 18 Wetting front migration for the embankment slope with remediation

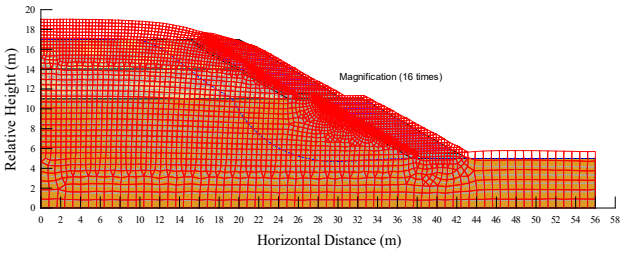

Figure 19 Deformed mesh due to changes in matric suction for the embankment slope with remediation

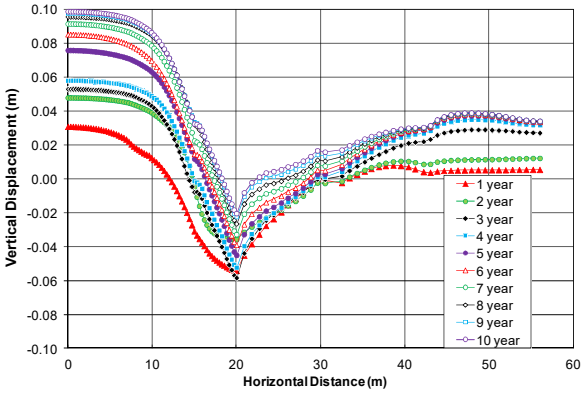

Figure 20 Change of heave with time along the ground surface for the embankment slope with remediation

Figure 17 also presents the minimum factor of safety with time for the cut slope with remediation. This figure illustrates that the minimum factor of safety for the slope with remediation decreases

gradually with time. The minimum long-term factor of safety for the slope with remediation is about 1.4 at the end of the modeling period. This illustrates that the proposed flexible reinforced structure approach should effectively increase the long-term stability of the cut slope.

4. CALCULATIONS OF POTENTIAL HEAVE USING THE OEDOMETER METHOD

4.1 General

Potential heave calculations were also conducted using the oedometer test method described in Section 2.1 with the migration of the wetting front data obtained in Section 3 for the embankment slope without remediation. The soil expansion properties for all materials were assumed to be the same and were obtained from typical laboratory test results provided by CSUST. The soil expansion properties are summarized in Table 2.

Table 2 Summary of soil expansion properties used in the calculations

Soil Expansion Property	Value
Percent Swell (%) (1)	17
Swelling Pressure from the CS Test (kPa)	250
Assumed m Value	0.4
Swelling Pressure from the CV Test (kPa)	51

Note: (1) Inundation pressure is approximately 1 kPa

4.2 Results of Calculations

Figure 14 indicates that most of the cross section could be saturated at the end of modeling period of 10 years. Therefore, to compute the maximum potential heave, it is assumed that the soils over the entire depth of potential heave will become fully wetted. The depth of potential heave is defined as the depth to which the overburden vertical stress equals or exceeds the swelling pressure of the soil (Nelson et al., 2001). The depth of potential heave was computed to be 2.5 meters using the soil properties shown in Table 2.

The soils throughout the entire depth of potential heave are divided into 5 layers, and the heave of each layer is computed. Table 3 shows the results of incremental heave computed for each layer. The total potential heave is the sum of the heave values calculated for all 5 layers. From Table 3 it is seen that the maximum potential heave is 101 mm.

Table 3 Potential heave calculations using the oedometer method for the slope without remediation

Depth to Bottom of Layer (m)	Interval (m)	Incremental Heave (mm)	Cumulative Heave (mm)
0.0			
0.5	0.5	50	50
1.0	0.5	26	76
1.5	0.5	15	91
2.0	0.5	8	99
2.5	0.5	2	101

5. DISCUSSION AND CONCLUSIONS

Field observation indicates that slope failures of expansive soil embankments usually occur in a shallow layer of the slope. The results of the numerical modeling are consistent with the observed depths of the slope failures. In addition, the numerical modeling shows that the minimum factor of safety for the cut slope without remediation reduces to below 1.0 within approximately 40 days after the start of the infiltration. This is also consistent with the general field observation of the slope failures.

The hypothetical expansive soil slope was assumed to be constructed with the flexible reinforced structure proposed by Zheng et al. (2009) to stabilize the cut slope. The maximum heave that is predicted to occur for the slope with remediation is reduced significantly compared to the original cut slope without remediation. The results of the SLOPE/W analysis show that the proposed flexible reinforced structure approach effectively increases the long-term stability of the cut slope.

Comparison of the water migration results indicates that the pore water pressure was reduced significantly for the slope with remediation due to the installation of the drain system. However, it is interesting to note that as shown in Figure 20 the inner edges of the drains at the horizontal distances of about 25 and 37 meters might heave less than the outer edges of the drains at the horizontal distances of about 30 and 42 meters. This could result in a negative slope of the drains along the cross section. The drains were assumed to be constructed horizontally in the model. Consequently, it is recommended that such drains be designed and constructed with an appropriate slope that considers the future movement of the slope.

For unsaturated soils, the modulus of elasticity is a function of a change in both matric suction and net normal stress. However, the increase in vertical stress because of the increase of the soil self-weight due to saturation is insignificant for expansive soils. Therefore, for analyzing volume change of expansive soils due to wetting, only the modulus of elasticity as a function of matric suction needs to be considered. The authors computed the values of modulus of elasticity from the oedometer test data in this study. The results of the computed E values using the oedometer test data indicate that oedometer test results can be used to determine reasonable E values. In view of the fact that the oedometer test most closely represents actual confinement conditions, it is concluded that the oedometer test is the preferred method for determining E. The confinement provided by the oedometer equipment also allows measurement of E to higher axial stress levels than either the triaxial or UC tests. Furthermore, because oedometer tests are more commonly performed than are triaxial or even unconfined compression tests, oedometer test results are more readily available.

A comparison of the predicted heave values at selected points along the cut slope without remediation using the numerical modeling method and the oedometer method is summarized in Table 4. The predicted heave obtained from the coupled SIGMA/W and SEEP/W analyses considers the swelling clay behavior due to changes in matric suction as the wetting front advances into the ground surface. The predicted heave from the numerical modeling method reflects a form of elastic rebound due to changes in modulus of elasticity. The predicted heave obtained using the oedometer method considers the expansion of the expansive soil due to hydration of adsorbed cations on the clay particles, in addition to the suction change of the soil. More research into the relationship between the two types of heave is necessary.

Table 4 Comparison of predicted heave obtained from the numerical modeling method and the oedometer method

Horizontal Distance, X	Predicted Heave from Numerical Modelling Method / Without Remediation (mm)	Predicted Heave from Oedometer Method / Without Remediation (mm)
X = 8.0 m	114	101
X = 20.0 m	110	101
X = 30.5 m	75	101

6. REFERENCES

Al-Mhaidib, A. I. (2006). "Swelling behavior of expansive shale, a case study from Saudi Arabia." In Expansive Soils - Recent Advances in Characterization and Treatment, A.A. Al-Rawas and M.F.A. Goosen, eds., Taylor & Francis Group, London, UK.

Al-Mhaidib, A. I. and Al-Shamrani, M. A. (2006). "Influence of swell on shear strength of expansive soils." Geotechnical Special Publication No. 148, Advances in Unsaturated Soils, Seepage, and Environmental Geotechnics, Proceedings of the GeoShanghai Conference, 160-165.

Bonner, J. P. (1998). Comparison of predicted heave using oedometer test data to actual heave. MS Thesis, Colorado State University, Fort Collins, Colorado, USA.

Chao, K. C. (2007). Design principles for foundations on expansive soils. Ph.D. Dissertation, Colorado State University, Fort Collins, Colorado, USA.

Darrg, A. A. (1984). Effect of swelling on the shear strength of Egyptian expansive soils. MS Thesis, Cairo University, Egypt.

Department of the Army, USA. (1983). Technical Manual TM 5-818-7, Foundations in expansive soils. Washington, DC.

Edil, T. B. and Alanazy, A. S. (1992). "Lateral swelling pressures." Proceedings of the 7th International Conference on Expansive Soils, Dallas, TX, 227-232.

Elkady, T. Y. and Abbas, M. F. (2012). "Shear strength behavior of highly expansive soil." Proceedings of the GeoCongress Conference, 2532-2541.

Feng, M., Gan, K. M., and Fredlund, D. G. (1998). "A laboratory study of swelling pressure using various test methods." Proceedings of the International Conference on Unsaturated Soils, Beijing, China, International Academic Publishers, VI, 350-355.

Fredlund, D. G. (2004). "Analysis of Decorah clay-shale at the Sandstone Ridge housing development in Cannon Falls, Minnesota." Project No. 98823-B.

Fredlund, D. G., Xing, A., and Huang, S. (1994). "Predicting the permeability function for unsaturated soils using the soil-water characteristic curve." Canadian Geotechnical Journal, 31(3): 533-546.

Fredlund, D. G. and Rahardjo, H. (1993). Soil Mechanics for Unsaturated Soils. Wiley, New York.

Fredlund, D. G., Rahardjo, H., and Fredlund, M. D. (2012). Unsaturated Soil Mechanics in Engineering Practice. Wiley, Hoboken, NJ.

Fredlund, D. G., Hasan, J. U., and Filson, H. (1980). "The prediction of total heave." Proceedings of the 4th International Conference on Expansive Soils, Denver, CO, 1-11.

Fredlund, D. G., Morgenstern, N. R., and Widger, R. A. (1978). "The shear strength of unsaturated soils." Canadian Geotechnical Journal, 15(3): 313-321.

GEO-SLOPE International, Ltd. (2007). GEO-STUDIO Software Package, Version 7.23. Calgary, Alberta, Canada.

Gilchrist, H. G. (1963). A study of volume change in highly plastic clay. MS Thesis, University of Saskatchewan, Saskatoon, SK.

Katti, R. K., Katti, D. R., and Katti, A. R. (2002). Behaviour of Saturated Expansive Soil and Control Methods. Revised and enlarged edition, Balkema, Netherlands.

Lambe, T. W. and Whitman, R. V. (1969). Soil Mechanics. Wiley, New York.

McCleskey, L. K. Jr. (2005). Experimental investigations to select stabilization methods to mitigate embankment desiccation cracks in order to reduce slope failures. MS Thesis, Department of Civil and Environmental Engineering, University of Texas at Arlington, Arlington, Texas, USA.

McKeen, R. G. (1992). "A model for predicting expansive soil behavior." Proceedings of the 7th International Conference on Expansive Soils, Dallas, TX, 1, 1–6.

Miao, L., Houston, S., Cui, Y., and Yuan, J. (2007). "Relationship between soil structure and mechanical behavior of an expansive unsaturated clay." Canadian Geotechnical Journal, 44: 126-137.

Miller, D. J., Durkee, D. B., Chao, K. C., and Nelson, J. D. (1995). "Simplified method for predicting heave in expansive soils." First International Conference on Unsaturated Soils, Paris, France.

Nelson, J. D. and Miller, D. J. (1992). Expansive Soils: Problems and Practice in Foundation and Pavement Engineering, Wiley, New York.

Nelson, J. D. and Chao, K. C. (2014). "Relationship between swelling pressures determined by constant volume and consolidation-swell oedometer tests." Proceedings of the UNSAT2014 Conference on Unsaturated Soils, Sydney, Australia.

Nelson, J. D., Overton, D. D., and Durkee, D. B. (2001). "Depth of Wetting and the Active Zone." Proceedings of the Geo-Institute Shallow Foundation and Soil Properties Committee Sessions at the ASCE 2001 Civil Engineering Conference, Houston, Texas, October.

Nelson, J. D., Reichler, D. K., and Cumbers, J. M. (2006). "Parameters for heave prediction by oedometer tests." Proceedings of the 4th International Conference on Unsaturated Soils, Carefree, AZ, 951-961.

Nelson, J. D., Chao, K. C., Overton, D. D., and Nelson, E. J. (2015). Foundation Engineering for Expansive Soils. Wiley, Hoboken, NJ.

Nelson, J. D., Chao, K. C., Overton, D. D., and Schaut, R. W. (2012). "Calculation of heave of deep pier foundations." Geotechnical Engineering Journal of the Southeast Asian Geotechnical Society and Association of Geotechnical Societies in Southeast Asia, 43(1): 12-25.

Ng, C. W. W., Zhan, L. T., Bao, C. G., Fredlund, D. G., and Gong, B. W. (2003). "Performance of an unsaturated expansive soil slope subjected to artificial rainfall infiltration." Geotechnique, 53(2): 143-157.

Porter, A. A. (1977). The mechanics of swelling in expansive clays. MS Thesis, Colorado State University, Fort Collins, Colorado, USA.

Reichler, D. K. (1997). Investigation of variation in swelling pressure values for an expansive soil. MS Thesis, Colorado State University, Fort Collins, Colorado, USA.

Sherif, M. M., Mazen, O., and Gergis, N. S.. (1984). "Behaviour of expansive soil during shear." Proceedings of the First National Conference on the Science and Technology of Buildings, Khartoum, Sudan, 557-562.

Thompson, R. W., Perko, H. A., and Rethamel, W. D. (2006). "Comparison of constant volume swell pressure and oedometer load-back pressure." Proceedings of the 4th International Conference on Unsaturated Soils, Carefree, AZ, 1787-1798.

Vu, H. Q. and Fredlund, D. G. (2006). "Challenges to modeling heave in expansive soils." Canadian Geotechnical Journal, 43: 1249-1272.

Wu, Lizhou and Huang, Runqiu. (2006). "Landslide mechanism and strengthening analysis of cutting slopes in expansive soil areas in China." The Geological Society of London, 1-5.

Zhan, L. T., Ng, C. W. W., and Fredlund, D. G. (2007). "Field study of rainfall infiltration into a grassed unsaturated expansive soil slope." Canadian Geotechnical Journal, 44: 392-408.

Zhan, T. L. T. and Ng, C. W. W. (2006). "Shear strength characteristics of an unsaturated expansive clay." Canadian Geotechnical Journal, 43: 751-763.

Zheng, J. L., R. Zhang, and Yang, H. P. (2009). "Highway subgrade construction in expansive soil areas." Journal of Materials in Civil Engineering, 21(4): 154-162.